

A 658-W VCSEL-pumped rod laser module with 52.6% optical efficiency

Xue-Peng Li(李雪鹏), Jing Yang(杨晶), Meng-Shuo Zhang(张梦硕), Tian-Li Yang(杨天利), Xiao-Jun Wang(王小军), and Qin-Jun Peng(彭钦军)

Citation: Chin. Phys. B, 2022, 31 (**8**): 084207. DOI: 10.1088/1674-1056/ac728f
Journal homepage: http://cpb.iphy.ac.cn; http://iopscience.iop.org/cpb

What follows is a list of articles you may be interested in

Large aperture phase-coded diffractive lens for achromatic and 16° field-of-view imaging with high efficiency

Gu Ma(马顾), Peng-Lei Zheng(郑鹏磊), Zheng-Wen Hu(胡正文), Suo-Dong Ma(马锁冬), Feng Xu(许峰), Dong-Lin Pu(浦东林), and Qin-Hua Wang(王钦华)

Chin. Phys. B, 2022, 31 (**7**): 074210. DOI: 10.1088/1674-1056/ac560c

High-efficiency asymmetric diffraction based on PT-antisymmetry in quantum dot molecules

Guangling Cheng(程广玲), Yongsheng Hu(胡永升), Wenxue Zhong(钟文学), and Aixi Chen(陈爱喜)

Chin. Phys. B, 2022, 31 (**1**): 014202. DOI: 10.1088/1674-1056/ac0422

Solar energy full-spectrum perfect absorption and efficient photo-thermal generation

Zhefu Liao(廖喆夫), Zhengqi Liu(刘正奇), Qizhao Wu(吴起兆), Xiaoshan Liu(刘晓山), Xuefeng Zhan(詹学峰), Gaorong Zeng(曾高荣), and Guiqiang Liu(刘桂强)

Chin. Phys. B, 2021, 30 (**8**): 084206. DOI: 10.1088/1674-1056/ac0696

High-efficiency terahertz wave generation with multiple frequencies by optimized cascaded difference frequency generation

Zhongyang Li(李忠洋), Binzhe Jiao(焦彬哲), Wenkai Liu(刘文锴), Qingfeng Hu(胡青峰), Gege Zhang(张格格), Qianze Yan(颜钤泽), Pibin Bing(邴丕彬), Fengrui Zhang(张风蕊), Zhan Wang(王湛), and Jianquan Yao(姚建铨)

Chin. Phys. B, 2021, 30 (**4**): 044211. DOI: 10.1088/1674-1056/abe3eb

Efficient manipulation of terahertz waves by multi-bit coding metasurfaces and further applications of such metasurfaces

Yunping Qi(祁云平) Baohe Zhang(张宝和), Jinghui Ding(丁京徽), Ting Zhang(张婷), Xiangxian Wang(王向贤), and Zao Yi(易早)

Chin. Phys. B, 2021, 30 (**2**): 024211. DOI: 10.1088/1674-1056/abd6fc

---

INSTRUMENTATION AND MEASUREMENT

A 658-W VCSEL-pumped rod laser module with 52.6% optical efficiency

Xue-Peng Li(李雪鹏)[1,4], Jing Yang(杨晶)[1,2,3,†], Meng-Shuo Zhang(张梦硕)[3], Tian-Li Yang(杨天利)[1,4], Xiao-Jun Wang(王小军)[1,2,3], and Qin-Jun Peng(彭钦军)[1,2,3]

[1] *Key Laboratory of Solid State Laser, Technical Institute of Physics and Chemistry, Chinese Academy of Sciences, Beijing* 100190, *China*

[2] *Key Laboratory of Functional Crystal and Laser Technology, Technical Institute of Physics and Chemistry, Chinese Academy of Sciences, Beijing* 100190, *China*

[3] *Institute of Optical Physics and Engineering Technology, Qilu Zhongke, Jinan* 250000, *China*

[4] *University of Chinese Academy of Sciences, Beijing* 100190, *China*

(Received 23 February 2022; revised manuscript received 17 May 2022; accepted manuscript online 24 May 2022)

A high-efficiency and high-power vertical-cavity surface-emitting laser (VCSEL) side-pumped rod Nd:YAG laser with temperature adaptability are demonstrated. The VCSEL side-pumped laser module is designed and optimized. Five VCSEL arrays are symmetrically located around the laser rod and a large size diffused reflection chamber is designed to ensure a uniform pump distribution. Furthermore, the absorbed pump power distribution of the rod is simulated to verify the uniformity of the pump absorption. Finally, a proof-of-principle experiment is performed in short linear cavity laser with single laser module. A continuous-wave output power of 658 W at 1064 nm is obtained, the corresponding optical-to-optical efficiency is 52.6%, and the power variations are ±0.7% over 400 s and ±3.1% over the temperature range from 16 °C to 26 °C. To the best of our knowledge, this is the highest output power and the highest optical-to-optical efficiency ever reported for VCSEL pumped solid-state lasers. By inserting a telescopic module into the cavity and optimizing the TEM_{00} mode volume, the average beam quality is measured to be $M^2 = 1.34$ under an output power of 102 W. The experimental results reveal that such a high power rod laser module with temperature stability is appropriate for field applications.

Keywords: rod laser, VCSEL-pumped, high-efficiency, temperature adaptability

PACS: 42.55.Xi, 42.60.Da, 42.60.Lh **DOI:** 10.1088/1674-1056/ac728f

1. Introduction

Vertical-cavity surface-emitting laser (VCSEL) has been proved as an excellent pump source for solid-state lasers for its remarkable low wavelength shift coefficient, all-direction-symmetrical beam profile and narrow beam divergence.[1–3] Especially the ∼ 0.06 nm/K wavelength shift coefficient makes it an ideal candidate pump source for the space and field applications.[4,5] However, compared with commonly used edge-emitting laser diode (LD), VCSEL chip has large emission area and relative low electro-optical conversion efficiency. Therefore, the power scaling of VCSEL side-pumped rod laser module faces two major challenges. The first is the junction temperature control of VCSEL array (VCSELA) with low electro-optical efficiency under large thermal generation and heat flow. The second is the coupling efficiency of VCSEL chip with large emission area to the rod laser module. Consequently, most previous demonstrations on the VCSEL pumped rod lasers were only several Watts output power.[6,7] Based on the VCSEL face-pumped slab architecture, 400-W level laser module was reported.[8,9] However, the face cooling design used in the slab lasers module cannot be directly transplanted in side-pumped rod module.

In order to overcome the aforementioned obstacles, we carefully study and optimize the parameters of VCSEL side-pumped rod Nd:YAG laser. We utilize several new approaches to obtain power scaling. First, the substrate material of VCSEL chip with high thermal conductivity is selected to reduce its own thermal resistance. Second, a vascularized macro-channel heat sink[10] is used in the thermal management of the VCSELA and the heat sink structure is also simulated, including the shortest distance from the chip to the channel, the transverse spacing and the vertical depth of the channel, the channel number, the size and position of the inlet and outlet of the heat sink, to realize an excellent heat removal and control the pressure loss of heat sink. Third, a five-fold symmetric pump structure is chosen and the structural parameters is simulated, such as the size of the crystal rod, the center distance from the VCSEL chip to the crystal rod, the inner diameter of the diffuse reflective chamber, the number of pump arrays, the inner diameter and outer diameter of the glass tube, to enhance the pump uniformity and the pump absorption efficiency. Consequently, a record-high power of 658 W and an optical–optical (o–o) efficiency of 52.6% from the VCSEL side-pumped rod laser is obtained for the first time. To the best of our knowl-

[†]Corresponding author. E-mail: yangjing@mail.ipc.ac.cn

© 2022 Chinese Physical Society and IOP Publishing Ltd

edge, this is the highest continuous-wave (CW) output power and the highest o–o efficiency for any VCSEL-pumped solid lasers.

Moreover, the output power stability has been tested, and the power fluctuations are ±0.7% over 400 s and ±3.1% in a temperature range from 16 °C to 26 °C. By inserting a telescopic module into the cavity and optimizing the fundamental mode volume, an average beam quality of $M^2 = 1.34$ is achieved under an output power of 102 W. Hopefully, the VCSEL pumped rod laser is a potential solution for the high average power applications in the complicated environment.

2. Design of the module

2.1. Design of VCSEL side-pumped laser module

A VCSEL pumped laser module with a relatively larger size of the laser gain medium and a large-diameter reflective chamber is one of the potential solutions for a highly efficient and high power VCSEL side-pumped laser module.[11,12] Figure 1 shows the cross section of the laser module. In order to obtain a large mode field and reduce the heat flux density in the gain medium, a 0.6-%-doped Φ8 mm×190 mm Nd:YAG rod is adopted. The side surface of the rod is roughened and the end facets of the rod are antireflection coated at 1064 nm. The rod is placed inside a cooling sleeve of glass tube. The cooling liquid flows rapidly the gap between the crystal and the glass tube. The inner diameter of the tube is $d_o = 11$ mm. The length of the annular flow is $L = 160$ mm. VCSEL is selected as the pump source due to its temperature insensitive property and narrow linewidth. Five linear VCSELA are arranged around the rod in five-fold symmetric directions with a total CW pump power of 1250 W at ∼ 808 nm. Each linear VCSELA with a size of 130.7 mm×4.7 mm contains 15 chips. Each chip from Laserconn (CS5-15-808-20W) has a size of 4.7 mm×4.7 mm and the beam divergence is 14.7° × 14.7° (full angle). To reduce thermal resistance of the VCSEL chip, the substrate material with high thermal conductivity is selected, which is similar to that of Ref. [8]. The Au-coated reflective chamber with a diameter of 44.4 mm has five slits that allow us to couple the emission of five linear VCSELA directly to the laser crystal rod, and the effective reflection area of this reflective chamber is more than 80%. Consequently, the reflective chamber distributes the pump beam uniformly through the crystal rod. The distance between the rod side-surface and the VCSEL emitting face of the pump source is $l = 26$ mm.

To estimate the gain uniformity of this laser module, the absorbed pump power distribution is simulated by ray-tracing at a pump power of 1250 W, as shown in the inset of Fig. 1. It can be found that the side-pumped structure results in a uniform high-gain area with a diameter of 5 mm with respect to the center of the rod and the total pump absorption efficiency η_a is around 85%.

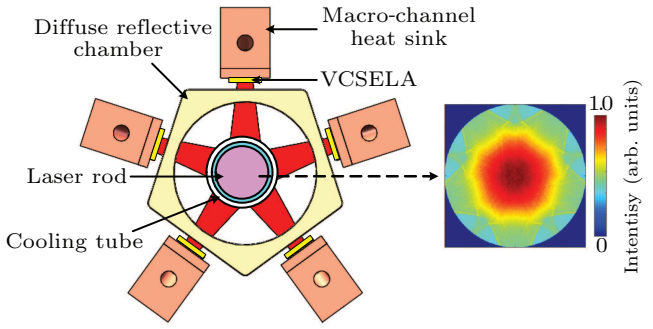


Fig. 1. Pumping configuration of the laser module. Inset: the simulation of the absorbed pump power distribution in the middle cross section of the Φ8 mm rod with $l = 26$ mm at total pump power of 1250 W.

2.2. Stability of pumping wavelength

The wavelengths of VCSEL are chosen carefully to match the absorption peak of the laser gain medium. High output power requires that an efficient thermal management to the VCSEL, which is closely related to the wavelength stability and the electro-optical conversion efficiency of the pump source. Since the wavelength of the VCSEL is insensitive to temperature changes, we select a macro-channel structure to cool the VCSEL array. To make optimal cooling, the heat sink structure is also computational fluid dynamic simulated. The following parameters are used in our heat sink. Fifteen fin groups are inserted in the copper heat sink, corresponding to the welding VCSEL chips. Each fin group contains five fins, the size of each fin is 8 mm×4 mm×0.8 mm and the period of the fins is 1.6 mm. The shortest distance between the VCSEL chip to the edge of the macro-channel is 3 mm. The inlet and outlet of the heat sink with a diameter of 5 mm are distributed at both ends of the heat sink. The water is used as the coolant. We simulate the temperature distribution on the surface of a single linear VCSEL array under 250-W pump power to verify the heat exchange performance of the macro-channel heat sink. The flow rate is 5 L/min and the coolant temperature at the inlet of the heat sink is 20 °C. The simulation result is shown in Fig. 2. It can be observed that the maximum temperature in the VCSELA is 26 °C and the minimum temperature at P near the inlet of heat sink is 24 °C. Thereby, the maximum temperature difference of VCSEL chips is 2 °C, which is only 0.12 nm for the corresponding wavelength drift on single linear VCSELA. This indicates that the macro-channel structure with fins has excellent heat removal performance and ensures the consistency of the output wavelength of the pump source. In our experiment, the pressure loss of this heat sink is less than 0.3 MPa at a flow rate of 5 L/min. Since it is macro-channel cooled VCSEL scheme, there is no longer need for a refined filter, deionized water and electric-conductivity control, which greatly reduces the complexity and maintenance cost of the thermal management system.

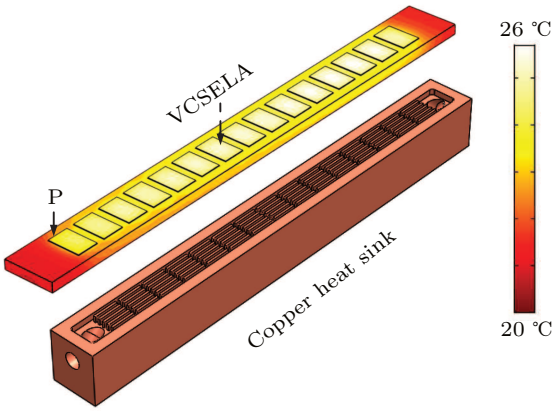


Fig. 2. Simulated temperature distribution on the surface of single linear VCSEL array with macro-channel heat sink for $W = 0.8$ mm and water flow rate 5 L/min at 20 °C under a pump power of 250 W.

Based on the optimized macro-channel heat sink, the wavelength characterization of the VCSEL chips is tested by a spectrometer (HR 4000, Ocean Optics) under CW operation. The wavelength of a linear VCSELA *versus* the water temperature at an output power 250 W is shown in Fig. 3. The shift of the central wavelength of the VCSELA is only 0.55 nm from 805.99 nm to 806.54 nm for the temperature spanning from 16 °C to 26 °C, corresponding to a wavelength shift coefficient of 0.055 nm/K, which is much smaller than 0.25 nm/K of the edge emitted laser diode (LD).[13] In addition, the wavelengths of five linear VCSELAs are measured at 20 °C. The central-wavelength change from 806.19 nm to 806.7 nm and the spectral full-width half-maximum (FWHM) range is 0.9 nm–1.4 nm. The normalized spectrum around 808 nm after the addition of the wavelengths of the five linear VCSELAs is sketched in the inset of Fig. 3. The center wavelength and FWHM of this added spectrum are 806.3 nm and 1.35 nm, respectively, suggesting that VCSEL with a center wavelength close to the absorption peak of the laser gain medium and a narrow linewidth is selected. The measured results show that the VCSEL is competent as a temperature-stable pump source for solid-state lasers.

The effective absorption efficiency of the Nd:YAG crystal is determined by the overlapping efficiency η_{over} between the Nd:YAG absorption spectrum and the VCSEL emission spectrum:[14]

$$\eta_{\text{over}}(T,\Delta\lambda) = \int \eta_{\text{abs}}(T,\lambda) S_{\text{pump}}(\lambda,\Delta\lambda)\,\mathrm{d}\lambda, \qquad (1)$$

where η_{abs} is the normalized spectra of the absorption ratio of the Nd:YAG crystal, which could find in Ref. [14]. A Gaussian profile is used to represent the pump spectrum S_{pump} for the VCSELA:

$$S_{\text{pump}}(\lambda,\Delta\lambda) = \sqrt{\frac{2}{\pi(\Delta\lambda)^2}} \exp\left[\frac{-2(\lambda-\lambda_0)}{(\Delta\lambda)^2}\right], \qquad (2)$$

where S_{pump} is a normalized emission spectral density of the VCSELA, T is the crystal temperature, $\Delta\lambda$ and λ_0 refer to the bandwidth and the center wavelength, respectively. Based on the data presented in Fig. 3, then, the calculated overlapping efficiencies η_{over} are 82.6%, 83%, and 83.5% at 16 °C, 20 °C, and 26 °C, respectively. Hence the variation of the overlapping efficiency is less than ±0.55%. The calculation results show that the VCSEL-pumped Nd:YAG crystal has high absorption efficiency and high temperature stability.

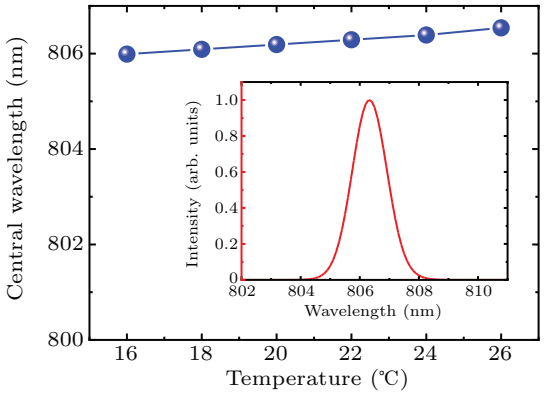


Fig. 3. Central wavelength of a linear VCSELA *versus* the temperature from 16 °C to 26 °C of the water at a fixed flux of 5 L/min and an output power of 250 W. The inset is the normalized spectrum around 808 nm after the summation of the wavelengths of the five linear VCSELAs at 20 °C.

3. Experimental investigation to the VCSEL side-pumped rod laser

In order to evaluate the lasing performance of the VCSEL side-pumped rod Nd:YAG laser module, a proof-of-principle experiment is implemented based on a short cavity multimode oscillator. The experiment setup is shown in Fig. 4. The laser cavity is made up of a high-reflective (HR) plane mirror M1 at 1064 nm and a plane output coupler M2 with transmission $T = 30\%$ at 1064 nm. The laser module is placed in the middle of the cavity and the total cavity length is 284 mm. The output beam enters a power meter (6K-W-BB-200×200, OPHIR) via a 45° HR mirror M3 at 1064 nm and an aperture for filtering stray light. Figure 5 depicts the evolution of the output power as a function of the incident pump power. It can be seen that the output power increases linearly with the incident pump power. At a pump power of 1250 W, a maximal laser output power of 658 W is generated, which is roughly two orders of magnitude higher than that in Ref. [7]. The corresponding o–o efficiency is 52.6%. Also visible in Fig. 5 is that the output power does not show any saturation or roll-off effect up to the maximum incident power, which seems to indicate higher power that may be achieved with higher pump power.

The wavefront distribution of the output beam is also measured at full output power by a wavefront sensor (HASO3 128-GE2, Axiom optics), as displayed in the inset at lower right of Fig. 5, which is similar to the one described in Ref. [15]. It is found that the peak-to-valley (PV) value of the wavefront is 1.16 μm and the root mean square (RMS)

is 0.26 μm after subtracting the defocus and tilt, since these low-order aberrations can be easily corrected by geometric optics.[16] It also can be seen from the measured result that the wavefront distortion is relatively small compared to Ref. [17].

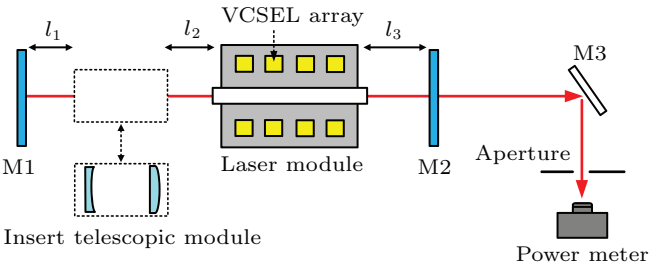


Fig. 4. Schematic diagram of the VCSEL-side-pumped rod Nd:YAG laser with a short cavity. M1: high-reflective mirror at 1064 nm; M2: output coupler; M3: 45° high-reflection mirror at 1064 nm.

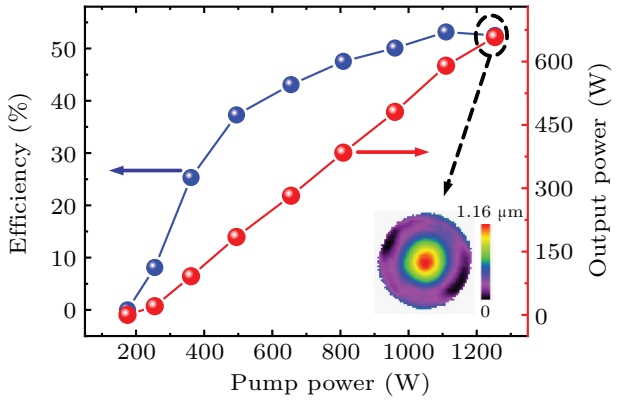


Fig. 5. Output power and o–o efficiency of the VCSEL-side-pumped 1064-nm rod Nd:YAG laser *versus* the pump power under CW operation. Lower right inset: measured wavefront distortion under VCSEL pump power of 1250 W.

In our previous experiment, we use a short cavity as a laser resonator to obtain a high average output power. However, owing to the existence of multiple transverse modes, the beam quality is not good. Therefore, we insert a telescopic module, which is in the place of black dashed frame in Fig. 4, and increase the length of the resonator, where the distances of each optical elements l_1, l_2, and l_3 are optimized to make it work in the thermal-near-unstable region.[18,19] The beam quality is tested using a commercial beam analyzer (Gentec Electro–Optics, BEAMAGE-M2). Under an output power of 102 W, the measured beam quality factors are $M_x^2 = 1.30$ at x axis and $M_y^2 = 1.37$ at y axis, corresponding to an average value of $M^2 = 1.34$, as shown in Fig. 6. The details of this work will be presented elsewhere.

The power-stability of the output power for this laser is experimentally investigated, as shown in Fig. 7. It is found that, at a coolant temperature of 20 °C, the output power variation is only ±0.7% over 400 s; The inset of Fig. 7 plots the output power *versus* the temperature. When the temperature changes from 16 °C to 26 °C, the variation of the output power is less than ±3.1%. The results indicate the precise temperature control device to the coolant is no longer needed, while the conventional diode-pumped lasers require a specific coolant temperature and the temperature fluctuation has to be strictly controlled within ±0.1 °C. As our previous report,[9] the excellent stability of the output power of the VCSEL-pumped Nd:YAG laser in a wide temperature range is result from the low wavelength shift of the VCSELA *versus* the temperature and the smaller change of the overlapping efficiency between the emission spectra of VCSELA and the absorption spectrum of the Nd:YAG crystal at different temperatures. Consequently, such a stable high-power laser module is very suitable for field applications even if harsh environmental conditions.

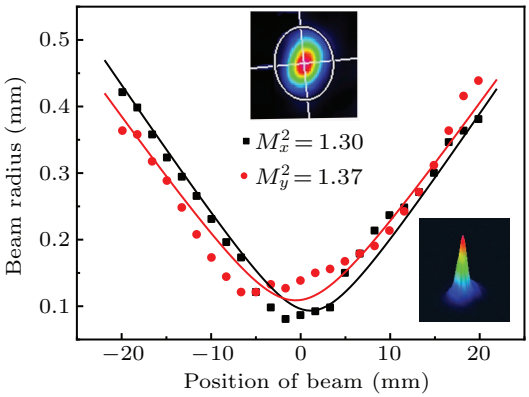


Fig. 6. Measured beam quality factors of the thermally near-unstable cavity with telescopic oscillator at an output power of 102 W. Upper inset: two-dimensional (2D) beam spatial profile. Lower right inset: three-dimensional (3D) beam spatial profile.

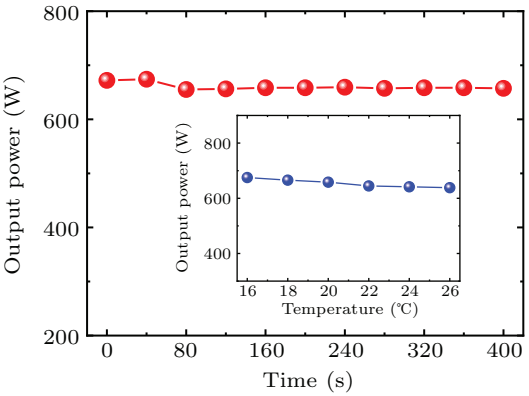


Fig. 7. Power-stability test at the highest output power over 400 s at 20 °C. Inset is the output power *versus* the temperature from 16 °C to 26 °C.

Moreover, in order to obtain higher pump power, diamond can be used as the substrate material of VCSEL chip to further reduce thermal resistance. For an application that needs to be operated in a low temperature environment, the coolant can be replaced with other fluid such as glycol and its solution and invar baseplate could be used to make the optical path stable. The lower temperature of the coolant indicates a lower junction temperature of a laser diode, which also means higher electro-optical efficiency. In this way, the VCSEL-pumped rod laser module with kW-class output capacity can be realized.

4. Conclusion

In summary, a temperature stable VCSELA side-pumped rod Nd:YAG laser with multi-hundred-Watt output power is designed and investigated for the first time. The output power and efficiency of the laser are greatly improved due to the optimization of the laser module structure and cavity parameters. As a result, a maximum CW output power of 658 W and a maximum o–o efficiency of 52.6% are obtained. To the best of our knowledge, this is the highest CW output power and the highest o–o efficiency for any VCSEL-pumped solid lasers. Meanwhile, the variations of the output power are measured to be less than $\pm 0.7\%$ over 400 s and $\pm 3.1\%$ over the temperature range from 16 °C to 26 °C. The experimental results reveal that the VCSEL side-pumped rod laser is appropriate for field applications and other scenarios which require a large temperature tolerance. Based on the laser gain module and telescopic resonator design, a laser oscillator with an average beam quality factor of $M^2 = 1.34$ is realized at an output power of 102 W and this work is in progress.

Acknowledgement

The authors would like to thank Prof. Da-Fu Cui for his helpful discussion in the manuscript modification.

References

[1] Morgan R A, Hibbs-Brenner M K, Marta T M, Walterson R A, Bounnak S, Kalweit E L and Lehman J A 1995 *IEEE Photon. Technol. Lett.* **7** 441

[2] Imada M, Chutinan A, Noda S and Mochizuki M 2002 *Phys. Rev. B* **65** 195306

[3] Hirose K, Liang Y, Kurosaka Y, Watanabe A, Sugiyama T and Noda S 2014 *Nat. Photon.* **8** 406

[4] Yu Z, Hou X, Zhou Q, Zhou C, Wang Z, Yang Y, Zhu R and Chen W 2013 *Chin. J. Lasers* **40** 0602003

[5] Bai J, Liu Y, Zhong C, Meng J, Shi J, Wang M, Meng J, Hou X and Chen W 2019 *Chin. J. Lasers* **46** 0101004

[6] Goldberg L, McIntosh C and Cole B 2011 *Opt. Express* **19** 4261

[7] Leeuwen R V, Xiong Y H, Seurin J F, Xu G Y, Miglo A, Wang Q, Xu B, Zou W X, Li D Z, Wynn J D, Khalfin V and Ghosh C L 2012 *Proc. SPIE* **8381** 83810I

[8] Li X P, Zhang X D, Yang J, Zhou Y X, Wang Y P, Di P C, Liu J, Liu K, Wang X J, Peng Q J and Xu Z Y 2020 *IEEE Photon. Technol. Lett.* **32** 434

[9] Di P C, Li X P, Yang J, Wang R J, Wang X J, Liu K, Cui D F and Peng Q J 2021 *IEEE Photon. Technol. Lett.* **33** 395

[10] Zhang X D, Li X P, Zhou Y X, Yang J and Liu J 2019 *Appl. Thermal Eng.* **162** 114212

[11] Furuta K, Kojima T, Fujikawa S and Nishimae J 2005 *Appl. Opt.* **44** 4119

[12] Cui Q J, Peng Q J, Zhang H B, Yang X Do, Bo Y, Guo X J, Zhou Y, Lu Y F, Cui D F and Xu Z Y 2008 *Chin. Phys. Lett.* **25** 3991

[13] Lee K, Kim Y, Lee S, Kwon J H, Gwak J S and Yi J 2013 *Appl. Opt.* **52** 5967

[14] Cho C Y, Huang T L, Cheng H P, Huang K F and Chen Y F 2016 *Opt. Express* **24** 1

[15] Song Y J, Xu Y Z, Meng S, Jing X X, Shao C F, Song Z X, Zong N, Wang Z M, Bo Y, Wang X J, Lin Z S and Peng Q J 2021 *Opt. Lett.* **46** 2425

[16] Yu X, Dong L Z, Lai B H, Yang P, Liu Y, Kong Q F, Yang K J, Tang G M and Xu B 2017 *Appl. Opt.* **56** 1730

[17] Wang C, Wei H, Jiang Y E, Wang J F, Qiao Z, Guo J T, Fan W and Li X C 2016 *Chin. Opt. Lett.* **14** 121402

[18] Yoshida S, Shimizu K, Tahil H and Tanaka I 2016 *IEEE J. Quantum Electron* **30** 160

[19] Feng Y, Bi Y, Xu Z Y and Zhang G Y 2003 *Proc. SPIE* **4969** 227